Nat. Volatiles & Essent. Oils, 2021; 8(4): 3222-3239

# Effect of Tri-Charged Boosting on Single Cylinder Four Stroke Diesel Engine at Different Compassion Ratio

**Bisane Rajesh[1], Kale Rajesh[2]**

*[1,2]Department of Mechanical Engineering, Rajiv Gandhi Institute of Technology, Versova, Andheri, Mumbai Maharashtra, India-400053*

*[1]St John College of Engineering and Management, Palghar Mumbai Maharashtra, India -401404*

**Abstract**

The paper presents the effects of crank driven supercharger, turbocharger and electric supercharger called a Tri-charger on a single-cylinder four-stroke diesel engine. Because the supercharger burns output power and the turbocharger has turbo-lag, the tri-charged system is designed to alleviate the drawbacks of both the supercharger and the turbocharger. The testing were carried out on a 1500 rpm constant-speed engine with varied load and compression ratios. The load increases from 0 to 12 kg in 2 kg increments, with a compression ratio of 16 to 20. The results show a considerable gain in volumetric efficiency as a result of super, turbo, and tri-charged boost air. Thermal efficiency, on the other hand, decreases at low and part load owing to super and turbocharger for all compression ratios. Furthermore, when operating at half and full load capacity, the engine equipped with a tri-charged boost enhanced thermal efficiency by 0.41 and 0.78 percent, respectively. The impact of tri-charging on engine emissions, CO, HC, and NOX is decreased by 0.38, 0.73, and 0.53 percent, respectively, for CR18. As a result, the tri-charger may be applied to a single-cylinder diesel engine without requiring any design changes, and engine performance and pollution criteria can be met.

**Keywords:** Naturally Aspirated Engine, Supercharged Engine, Turbocharged Engine, Tri-Charged Engine, Engine Performance, Emission Characteristics.

## 1. Introduction

Improving economy, power capacity, and lowering pollutants such as NOX, CO2, HC, and others are significant challenges for vehicle manufacturers [1]. Because of the low decarburization of combustible products, the transportation industry is the second-largest contributor to global greenhouse gas emissions [2]. The greatest choice for implementing without modifying the engine architecture is a multi-stage boosting system. The multi-stage boosting system employs more than two chargers (boosting devices) in order to increase power and performance [3]. As a result, a tri-charged boosting system is developed without modifying the engine's architecture. The term "tri-charged" refers to multi-stage boosting. To alleviate the problem of turbo-lag, a crank-driven supercharger powered by engine output provides an initial charge to the turbo driven on the exhaust. As the engine speeds up, the exhaust gases produced are sufficient to power the turbocharger. The tri-charge boosting system is completed with an electric-driven supercharger that supplies boost air [4] different arrangements for putting boosting systems in place [5]. The exhaust from the engine impinges on the blades of two turbocharger turbines in a parallel configuration, and compressed air is fed to the inlet at a single point.

This configuration is applicable to multi-cylinder engines. HP turbine and LP turbine are connected in sequence in a series type setup. It has better traction than parallel type but requires more difficult installation, generates more heat, and the HP turbine consumes the majority of the exhaust gases [6]. The combined super-turbo setup is the third kind. The LP supercharger is positioned on the output shaft, making maintenance and installation easier, whereas the HP turbocharger is powered by exhaust gases. It produces a respectable result but uses engine power and suffers from turbo-lag [7-8]. Implementing a tri-charged system addresses the issues of power loss and turbo-lag and is seen as a suitable solution. It is critical to pick an adequate turbocharger for the engine's capacity [9-10]. If the turbo has a flow capacity that is either too large or too little, it may cause variability in the engine's operation, resulting in poor engine performance [11-13]. According to Feng Y. et al. [14], the intake pressure state is transitory at low engine speeds of roughly 2000 rpm and steady at high engine speeds of around 4000 rpm. However, using turbochargers alone at low engine speeds is ineffective. The turbo in a twin-scroll system is heated to a high temperature and feeds hot air to the engine, resulting in increased NOX emissions. It necessitates the use of extra cooling devices such as an intercooler, oil coolant, and shielding [15-16]. More pipes are necessary as a result of the addition of an intercooler or radiator, and engine construction becomes more difficult [17]. All of the systems stated above are found in the turbocharger, and the largest issue with the turbocharger is turbo-lag. The turbocharger does not operate because sufficient boosting pressure is not achieved [18-19]. To address the issue of turbo-lag, Song K et al. [20] created a variable geometry turbocharger (VGT). In VGT, moveable vanes are replaced with fixed vanes to optimise air and fuel consumption mass flow by altering angles on the turbine blades to regulate exhaust gas flow [21]. Because of the wider flow area in VGT, the exhaust gas velocity is reduced, resulting in lesser intake boost at low and middle engine speeds. Another disadvantage of VGT is its slow acceleration from a standstill and higher total cost. VGT turbine expansion ratio rises with power as intake pressure rises [23-24]. The turbocharger, in conjunction with EGR, removes or reduces the need for boost to some extent, lowering fuel usage to produce boost air [25-26]. However, the EGR system is only effective at a 5% rate of reduction in NOX emissions. [27-29], Thus, a supercharger is the optimum choice to employ in conjunction with a turbocharger, and it may be installed in two ways: one manually crank driven, and the other using electricity from a battery. The advantage of a crank driven supercharger is that it has an excellent responsiveness to changeable loading situations since it works in response to an increase or reduction in load with a stable compression ratio, resulting in no turbo-lag. [30-32]. the mechanically crank powered supercharger, on the other hand, uses a large amount of output power. It has a supercharging limit and frequent belt slide after more than 30000 km. Experiments on the high-pressure multi-stage boosting system, i.e. turbo-super system at varied super pressures, reveal that utilising a supercharger with optimal throttling circumstances improves efficiency [33-35]. Zhu et al. [36] discovered that the supercharger, ASY turbocharger, and VGT are heavily employed in SI engines to increase the speed and power of multi-cylinder engines. Zhu et al. [36] discovered that the supercharger, ASY turbocharger, and VGT are heavily employed in SI engines to increase the speed and power of multi-cylinder engines. Buchman et al. [37] devised a system for turbocharging single-cylinder, four-stroke engines in which an air capacitor connected in series between the turbocharger compressor and the intake manifold protects the product from the turbocharger outlet [38]. Transportation vehicles consume more than 70% of fossil fuels and contribute to increased air and noise pollution. [39] Koniuszy et al. The Indian government has begun to accelerate the adoption and manufacture of electric cars (EVs), with a goal of 30 percent (EVs) by 2030 and India being an all-EVs market by 2040. Faster adoption of EVs is difficult due to several hurdles, including the fact that EVs are more expensive than gasoline and diesel cars, and the battery is a vital component of an engine [41]. Currently, all EVs employ lithium-ion batteries, which are excessively costly and have limits in terms of long-distance travel and a life span of four years. As a result, deploying EVs in India will take some time since adequate charging station infrastructure is lacking [42]. However, when compared to e-tractors and e-trucks, the adoption of e-bikes and e-cars is extremely feasible. The reason for this is that tractors and trucks need torque of greater than 300-400 N-m to perform farm tasks such as ploughing, harrowing, rotary harrowing, sowing, rolling, and so on. Along with vehicle electrification, about 8% of mild hybrid electric cars (MHEV) and 20% of full hybrid electric vehicles (FHEV) are advantageous in terms of PM and HC reduction [43]. As a result of the reduction in ignition delay, a turbocharger with tri-charged technology can cut fuel consumption at part load by around 2% [44]. Much study has been done on performance increase on multi-cylinder diesel engines employing stand-alone supercharger and turbocharger or in a combination of super-turbo with varied layouts, as seen by the literature referenced above. There is potential for creating a tri-charged system, particularly for a single-cylinder engine suitable for tractor use, which improves brake power, decreases fuel consumption, and reduces NOX emissions to meet demand. The current study compared the performance of a single-cylinder diesel engine to that of a supercharged, turbocharged, and tri-charged engine at a constant speed of roughly 1500 rpm with 0 kg, 2 kg, 4 kg, 6 kg, 8 kg, 10 kg, and 12 kg loading circumstances. Compression ratios of 16, 18, and 20 are used to test emissions and engine performance for each adjustment. Figure no.1 provides a revised summary of c-super, turbo, e-super, and tri-charged systems.

**Figure 1: Modified layout of (a) Crank Supercharged (b) Turbocharged (c) Twin-charged (d) Tri-charged Engine**

**(a) C-Supercharged System**

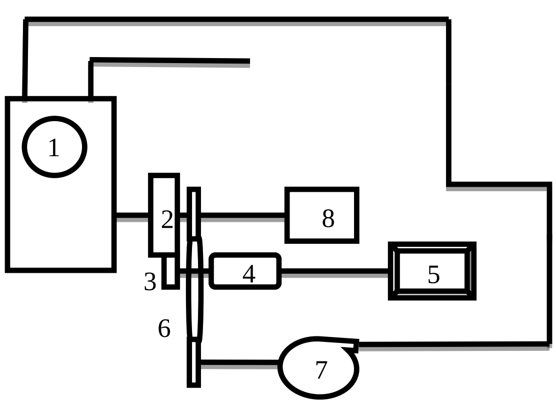


1. Single Cylinder Four Stroke Diesel Engine 2. Flywheel 3.Starter Wheel 4. Starter Motor 5. Battery 6. Pulley Belt arrangement 7. Supercharger, 8. ED Current Dynamometer

**(b) Turbocharged System**

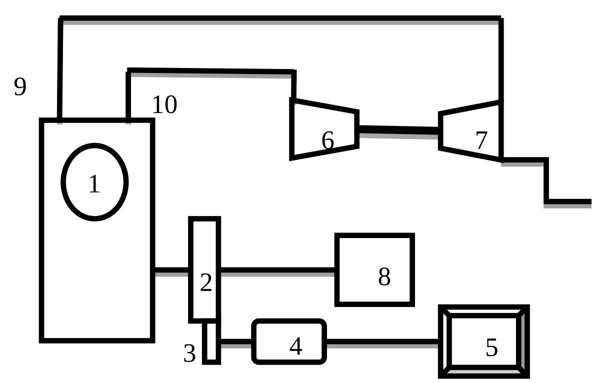


1. Single Cylinder Four Stroke Diesel Engine 2. Flywheel 3.Starter Wheel 4. Starter Motor 5. Battery 6. Turbine 7. Compressor 8. ED Current Dynamometer 9. Intake Manifold 10. Exhaust Manifold

| (c) Twin-charged System | (d) Tri-charged System |
|---|---|
| 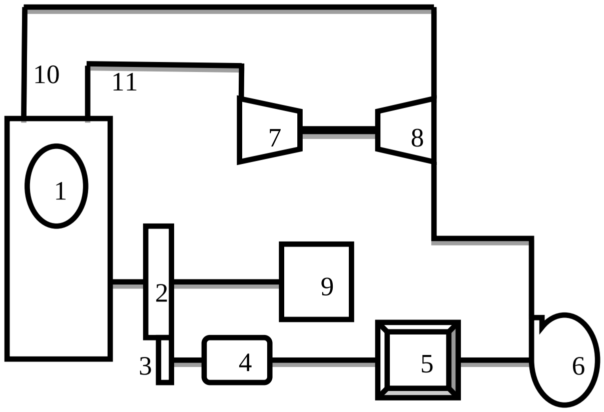  1. Single Cylinder Four Stroke Diesel Engine 2. Flywheel 3.Starter Wheel 4. Starter Motor 5. Battery 6. E-Supercharger 7. Turbine 8. Compressor, 9. ED Current Dynamometer 10. Intake Manifold, 11. Exhaust Manifold | 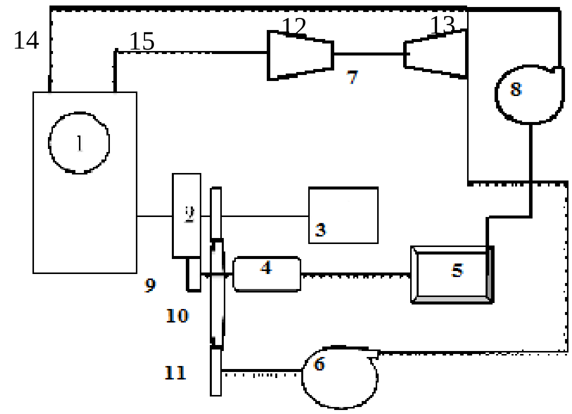  1. Single Cylinder Four Stroke Diesel Engine 2. Flywheel 3. Eddy current Dynamometer 4.Starter Motor 5. Battery 6.C- Supercharger 7. Turbocharger 8. E- Supercharger 9. Starter Wheel 10. Belt 11. Pulley 12. Turbine 13. Compressor 14. Intake Manifold 15. Exhaust Manifold |

## 2. Experimental Setup and Processes

**Figure 2. Layout C-Super, E-Super, Turbo and Tri-Charged System**

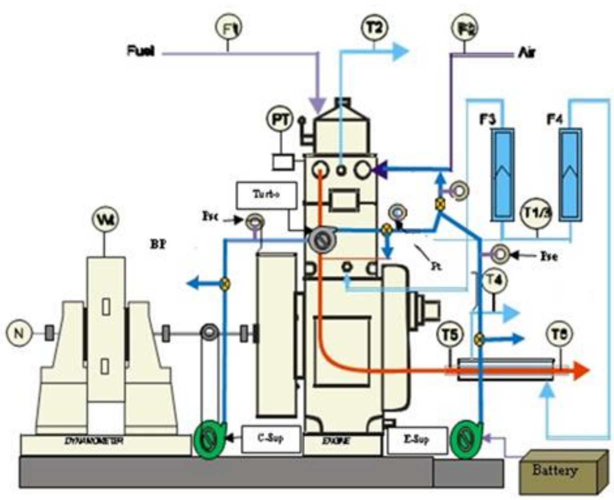


**Figure 3. Single Cylinder 4-Stroke VCR (Computerised) Test Rig**

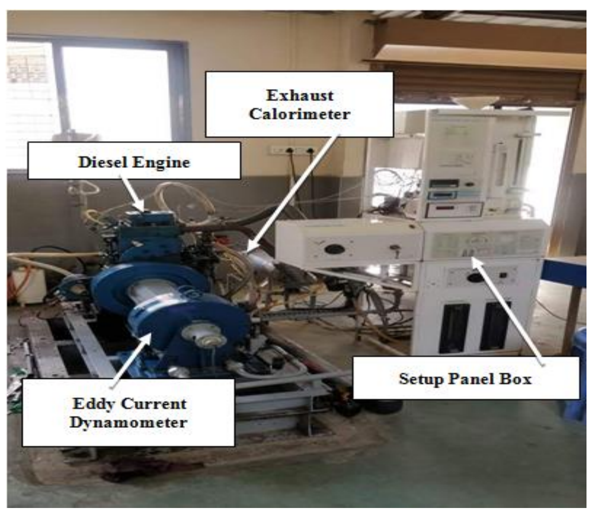


The investigations were carried out at the dedicated Research Associated Lab (RAL) at Apex Innovations Pvt. Ltd. Sangali, Maharashtra, India. . The crank driven supercharger, turbocharger and electric supercharger combined assembly is shown in Fig.2**.** The setup consists of a single-cylinder, four-stroke, diesel engine connected to an eddy current dynamometer, computerised model-224 shown in

Fig.3. The test setup provided with necessary sensors for combustion pressure and crank-angle measurements. These signals from respective sensors interfaced to the computer through engine indicator for P-θ diagrams. The setup has a stand-alone panel box consisting of the air box, fuel tank, water manometer, and burette as a fuel measuring unit. Rotameters are provided for cooling water and calorimeter water flow measurement. The setup enables the study of engine performance for brake power, indicated power, frictional power, BMEP, IMEP, brake thermal efficiency, indicated thermal efficiency, Mechanical efficiency, volumetric efficiency, specific fuel consumption, A/F ratio and heat balance. 'Enginesoft' is used to interface the engine performance result and analysis. A computerized diesel injection pressure measurement is also provided. The exhaust gasses emissions are measured by exhaust gas analyser (AVL DIGAS 444N), respective parameters, measurement, and resolution shown in Table 1.

**Table 1: Exhaust Gas Analyser (AVL DIGAS 444N)**

| **Parameters** | **Measurement** | **Resolution** |
|---|---|---|
| CO | 0-15 % Vol | 0.001 % Vol. |
| HC | 0-3 % Vol | 4 % Vol |
| CO2 | 0-5 % Vol | 6 % Vol |
| O2 | 0-25 % Vol. | 0.01 % Vol. |
| NOX | 0-5000 ppm | 1 ppm |
| Engine Speed | 400-6000 rpm | 1 rpm |
| Oil temperature | 0 ºC- 125 ºC | 1 ºC |
| Lambda (λ) | 0 -9.999 | 0.001 |

The experimental setup was developed with the help of three main assemblies are as follows.

**2.1 Crank Driven Supercharger**

The crank driven supercharger is an air blower attached to the crankshaft at the back of the engine by a belt and pulley system that transfers power from the crankshaft to the supercharger **(Refer Fig 4)**. The torque generated by supercharging is measured using a torque metre located at the crankshaft pulley's end. The pressure gauge and temperature measuring sensor were used to measure the supercharger's inlet pressure and temperature (IST AG platinum temperature sensors). The mass flow rate fluctuates with the engine's loading state and is monitored accordingly by the manometer.

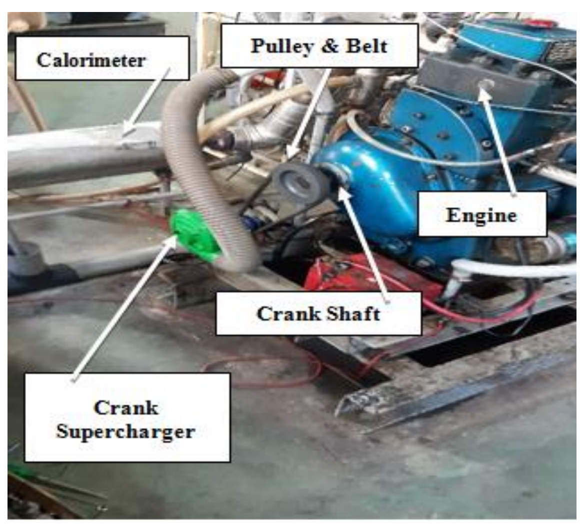


**Figure 4. Crank Driven Supercharged Engine Setup**

The following mathematical equation expresses the relationship between supercharging pressure and temperature.

$$\frac{T2}{T1} = \left(\frac{p2}{p1}\right)^{\gamma-\frac{1}{\gamma}} \quad (1)$$

### 2.2 Exhaust Driven Turbocharger

A turbocharger is attached to the engine's exhaust pipe using a specially designed clamper with dimensions the same as the exhaust pipe **(Refer Fig. 5).** The housing connects the turbocharger at the entry of exhaust hot gasses and waste-gate to escape the unwanted gases. The temperature and pressure after the turbocharger were measured. After turbocharging, the gases were allowed to pass through the calorimeter. The turbocharger's efficiency is the conversion of exhaust energy into work required for compression and is calculated using the following expression.

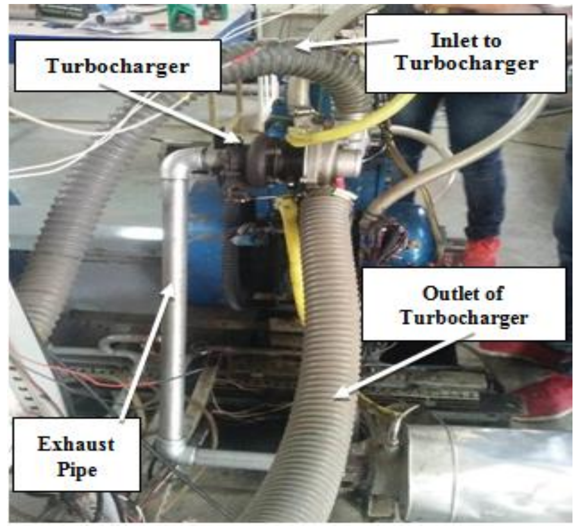


**Figure 5. Turbocharged Engine Setup**

$$\eta Tc = \frac{mco.e_{p,Com}\left(Tci\,\frac{Pco}{Pci}\right)}{mTi.e_{p,Exp}\left(T_{Ti}\frac{PTi}{PTo}\right)} \quad (1)$$

### 2.3 Electric-Supercharger

A supercharger runs through the power of 12V battery (**Fig. 6**). An orifice air control valve controls the mass of air at around 50 % opening optimum. The pressure gauge and temperature sensor were attached after the valve to measure the exit pressure and temperature of the electrically driven supercharger.

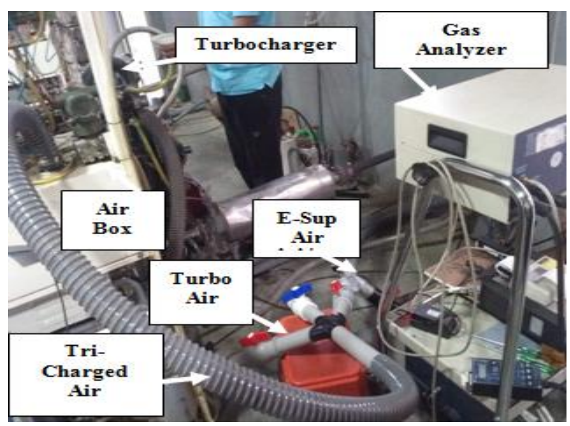


**Figure 6. Electric Driven Supercharged Engine Setup**

### 2.4 Tri-charger

The tri-charged assembly (**Refer Fig. 7**) in this a supercharger (Air Blower) was assembled to the crankshaft through the belt and pully mechanism. A turbocharger is attached to the exhaust pipe to run on the exhaust gas, and an electric supercharger runs by 12V battery. The combined super, turbo and tri-charged boost air is maxed at a specially designed Y join, further supplied to the intake. The pressure gauges and temperature sensors are mounted at the combined c-super, e-super and turbocharged Y pipe exit. The corrected mass flow rate after the combination of the tri-charged system is defined using the following relation.

Pr. & Tr. = Referential pressure in (bar) & temperature in (°C) which is equal to the atmospheric pressure and temperature

Pa. & Ta. = Actual pressure in (bar) & temperature in (°C) which is inlet to the engine after tri-charging at different modifications as super and turbo

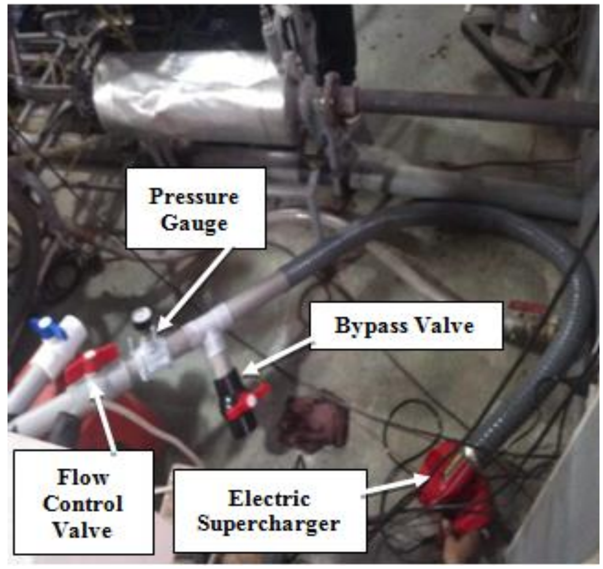

**Figure 7. Tri-charged Engine Setup**

$$m_{corrected} = m_{actual} \frac{P_r}{P_a} \sqrt{\frac{T_a}{T_r}} \quad (2)$$

Initially, the test was carried out on a conventional single-cylinder four-stroke diesel engine at a compression ratio of 18, further modified to a supercharged engine with the same 16, 18 and 20 CR. Similarly, supercharger replaced by turbocharger and test was conducted and lastly tested conducted on combined tri-charged engine and results are compared for a different compression ratio of 16, 18 and 20 at variable load from 2 kg to 12kg.

## 3. Results and Discussion

This section compares the performance evaluation and emission analysis on the conventional engine compared with the crank driven supercharger, e-supercharger, turbocharger, and tri-charger. Experiments on single-cylinder conventional diesel engines are conducted first at a constant speed of 1500 rpm with 2 kg, 4 kg, 6 kg, 8 kg, 10 kg, and 12 kg of loading conditions. Then the conventional engine was modified with a crank driven supercharger with the same speed and load, further modified by turbocharger and tri-charger with the same speed and loading conditions.

### 3.1 Effects on Brake Specific Fuel Consumption: [BSFC]

**Fig. 8** shows the variation of BSFC with a change in loading of the engine. The lowest value of the BSFC represents that the engine is efficient. The experimental result shows a significant increment in the BSFC compared to the naturally aspirated engine. At low load, BSFC increases from 0.91 Kg/kWh to 0.94 Kg/kWh average of all 16 CR, 18 CR, and 20 CR, operate with supercharger. The average increase in BSFC is 0.93 Kg/kWh, slightly lower than the supercharger and further reduced to 0.896 Kg/kWh with tri-charger when operating with a turbocharger. Whereas there is not much variation in BSFC found at a partial load of 4 to 6 kg for turbo and tri-charger compared to the supercharger, the best operating condition for partial load is observed at the turbocharged engine with a compression ratio of 18 for 6 kg

**Figure 8. Load vs. BSFC**

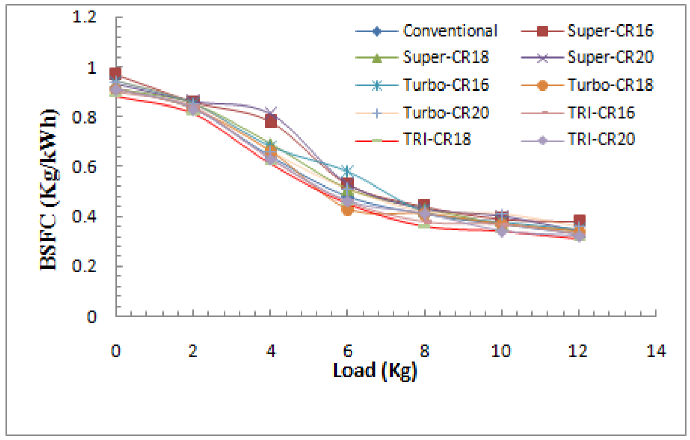


load. For a full load, the best operating condition is a tri-charger with CR 18 at 12 kg load. Therefore the tri-charging technology tends to reduce the BSFC compared to the conventional, super and turbocharged engine.

**3.2 Effects on Brake Thermal Efficiency: [BTHE]**

**Figure 9. Load vs. BTHE**

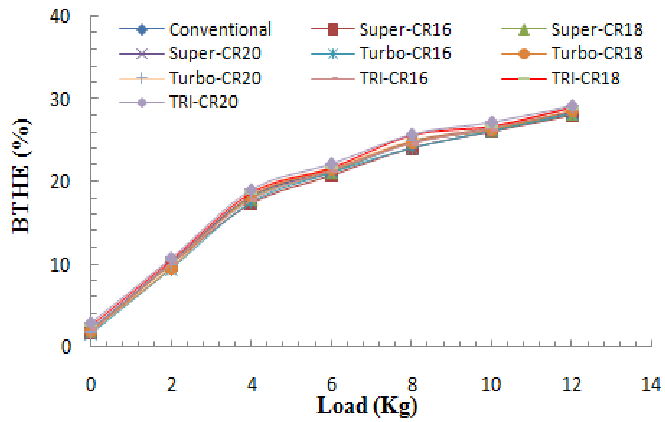


The engine thermal efficiency at full load condition represents the heat to power ratio of the engine. Through experimentation, brake thermal efficiency for CR 16, 18 and 20 decreases from 2.11 % to an average of 1.86 % at supercharged conditions. Further, BTHE decreases from 21.24 % to 21.09 % at turbocharged mode and tri-charged from 28.32 % to 28.21 %; thus, the power tends to increase capacity with the penalty of fuel consumption for all CR. When the engine operates at turbocharged boost air, there is a slight fall in BTHE at a low load of 2 kg, from 10.24 % to 9.66 %, whereas it is increasing at part and full load 21.41 % and 28.57 %, respectively. Also, there is a significant increment in the BTHE when run at tri-charged modification to 10.47 %, 21.73 % and 29.03 % for CR16, CR18 and CR20. The best BTHE is 29.13 % at tri-charged with CR20, whereas for all CR 16 to 20, the BTHE is higher than conventional, super, and turbocharged modification due to reduction in ignition lag and optimized boost charge. **(Fig.9)**

**3.3 Effects on Volumetric Efficiency: [VE]**

**Figure 10. Load vs. VE**

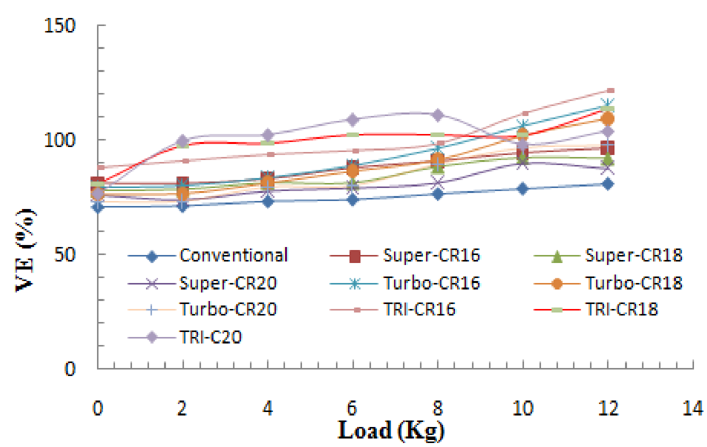


The volumetric efficiency of the engines is associated with the mass density of the air-fuel mixture drawn into the cylinder. Like a supercharger, turbocharger and tri-charger provide boost air to the engine. Therefore, there is a significant increment in the volumetric efficiency when operating at low, part and full load capacity with variation in compression ratio. For 12 kg of full loaf capacity, the VE increases from 81.17 % to 96.77 % for super CR16, 115.65 for turbo CR 16 and 121.88 % for tri-charged CR 16.Thus the higher value of VE at a compression ratio of 16 for super, turbo, and tri-charged engine (**Fig. 10**).

## 4. Emission Analysis

### 4.1 Emission Characteristics: CO

**Figure 11. Load vs. CO**

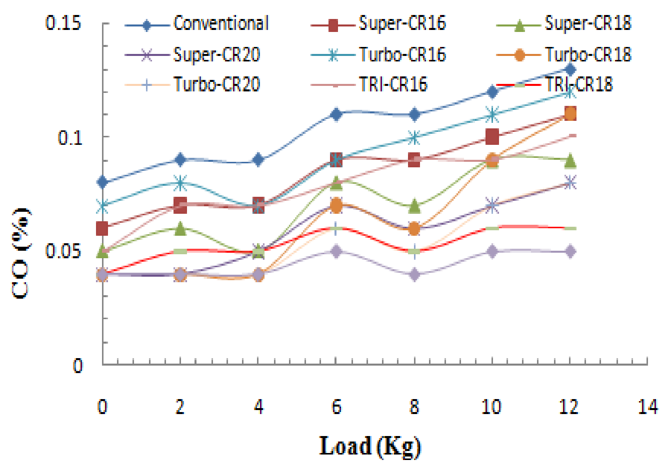


The variation of CO produced from the conventional engine compared with supercharged, turbocharged and tri-charged engines in (**Fig. 11).** Boosting air affects the air-fuel ratio, density, and atomization of fuel; thus, CO emissions are reduced significantly. The CO is reduced significantly when the engine operates at modifying a supercharger, turbocharger, and tri-charger for all compression ratios. At a low load of 2 kg, CO reduced from 0.09 % vol. to 0.04 % vol. at super, turbo and tri-charged mode for compression ratio as 20. Similarly, CO emissions are reduced at part load from 0.11% vol. to 0.07 % vol by a supercharger, 0.06 % vol. Due to turbocharging and 0.05 % vol by tri-charging. A significant change in CO emissions is observed when the engine operates at full load capacity, and the CO is reduced from 0.13 % vol. to 0.08, and 0.05 % vol. at super, turbo and tri-charged engine. Thus based on the obtained results, the CO emissions of diesel engines can be reduced by the boost tri-charging.

### 4.2 Emission Characteristics: HC

**Figure 12. Load vs. HC**

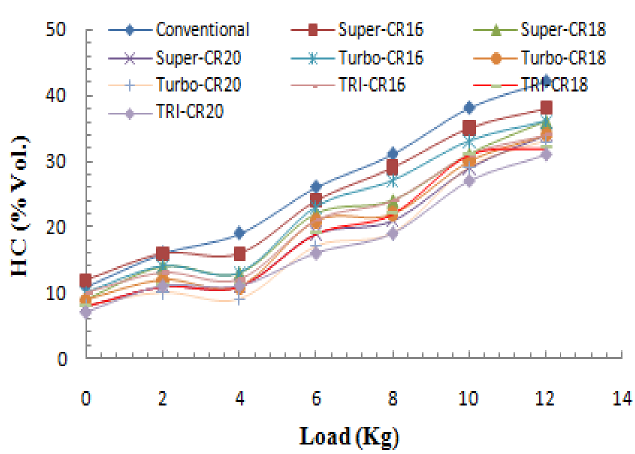


At three different compression ratios, the influence of tri-charged boost pressure on the HC emissions index was studied. The rise in UHC at decreasing O2 concentrations is typical of this dilution-controlled LTC regime [11, 12]. UHC emissions are generally lower with larger loads, with the exception of when the global equivalency ratio approaches or surpasses 1. **(Fig. 12)** compares the HC emissions of a regular engine to those of a supercharged, turbocharged, and tri-charged engine operating at varied loading circumstances and compression ratios. The results show a considerable decrease in HC as a result of supercharging, turbocharging, and tri-charging technologies. At 2 kg loading condition, the HC was lowered from 16 ppm to 11 ppm by supercharger at CR 20, 8 ppm by turbocharger, and 7 ppm by tri-charger. Due to super, turbo, and tri-charging, HC was lowered from 26 ppm to 19 ppm, 17 ppm, and 16 ppm at part load, respectively. HC was also lowered from 42 ppm to 31 ppm at full load, indicating that boosting air density as a boost charge is effective in lowering HC emissions.

### 4.3 Emission Characteristics: $NO_X$

**Figure 13. Load vs. $NO_X$**

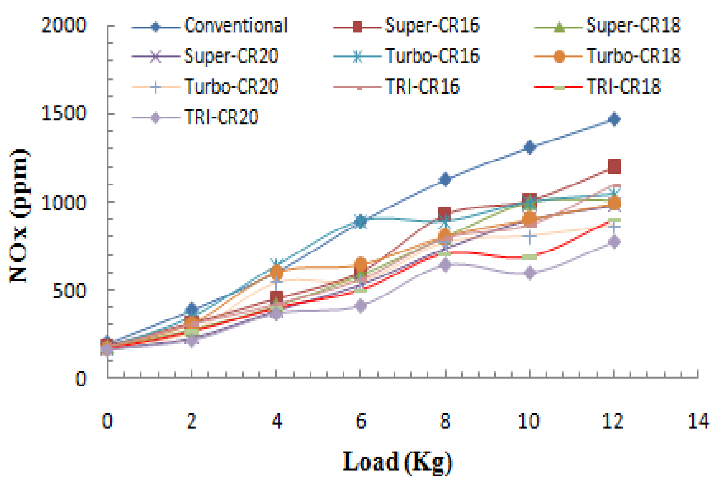


Load Vs, $NO_X$ emissions characteristics, are shown in **Fig. 13.** There is not much variation in $NO_X$ at the no-load condition for CR 16, whereas, at part load capacity, the $NO_X$ reduced significantly from 887 ppm to 532 ppm, 557 ppm, and 411 ppm when operating at super, turbo and tri-charged mode. An excellent change in $NO_X$ was observed when operates at the super, turbo and tri-charged modification from 1466 ppm to 977 ppm, 866 ppm and 775 ppm for CR 20. Thus increase in boost pressure and compression ratio results in a reduction in NOX emissions.

## 5. Combustion Analysis

### 5.1 Engine Details

IC Engine set up under test is research diesel engine having power 3.50 kW @ 1500 rpm which is single cylinder, four stroke , constant speed, Cylinder Bore 87.50(mm), Stroke Length 110.00(mm), Connecting Rod length 234.00(mm), Compression Ratio 18.00, Swept volume 661.45 (cc)

### 5.2 Combustion Parameters

Specific Gas Const (kJ/kgK): 1.00, Air Density (kg/m^3): 1.17, Adiabatic Index: 1.41, Polytrophic Index: 1.05, Number of Cycles: 10, Cylinder Pressure Reference: 5, Smoothing 2, TDC Reference: 0

### 5.3 Performance Parameters

Orifice Diameter (mm): 20.00, Orifice Coefficient of discharge: 0.60, Dynamometer Arm Length (mm): 185, Fuel Pipe dia. (mm): 12.40, Ambient Temp. (Deg C): 27, Pulses Per revolution: 360, Fuel Type: Diesel, Fuel Density (Kg/m^3): 722, Calorific Value of Fuel (kj/kg): 38850. The measuring instrument, range, and accuracy.

**Table 4 Measuring instrument, range and accuracy**

| Measuring instruments | Range | Accuracy |
|---|---|---|
| Piezo sensor: Make PCB USA, Combustion | 350 bar | $\pm 1$ **bar** |
| Speed sensor: Make Kubler Germany, Resolution 1º | 0-5500 rpm | $\pm 1$ **rpm** |
| Temperature transmitter: Make ABUSTEK USA, Type two wire, Input RTD PT100, Thermocouple, | 0-100 ºC<br>4–20 mA | $\pm 1$ **ºC**<br>$\pm 0.5$ **mA** |
| Load sensor: Make VPG Sensotronics | 0-50 Kg | $\pm 0.5$ **Kg** |
| Fuel flow transmitter: Make Yokogawa Japan, DP transmitter) | 0-500 mm WC | $\pm 1.5$ **mm** |
| Air flow transmitter: Make Wika Germany, Pressure transmitter, | 0-250 mm WC | $\pm 1$ **mm** |
| Rotameter & Calorimeter: Make Eureka, Engine cooling, | 40-400 LPH<br>25-250 LPH | $\pm 5$ **LPH**<br>$\pm 5$ **LPH** |
| Smoke analyser AVL 437 Smoke Meter, Opacity 0.1 %, Operating Temperature:5ºC to 50º C | Capacity 0-100 % | $\pm 0.1\ \mathbf{m} - 3$ |

**Figure 14. Variation of Cylinder Pressure**

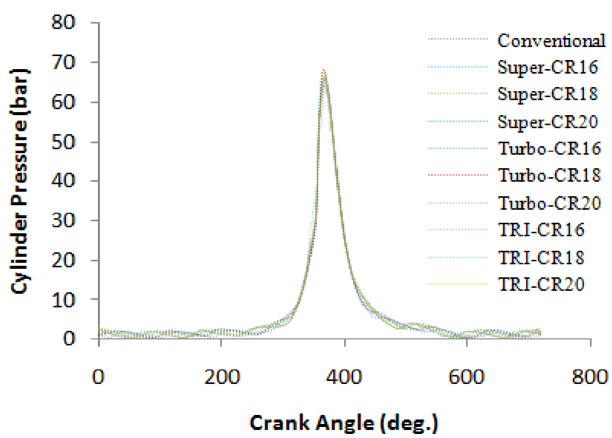


All the tests were carried out at six different loads viz. 2 kg, 4 kg, 6 kg, 8 kg, 10 kg, 12 kg, and at a constant speed of 1500 rpm with a suitable combination of intake pressure and temperature and exhaust backpressure. To understand the overall effect of tri-charged with different boost devices and compression ratios was investigated. It is found that the engine tends to knock at 55 º BTDC fuel injection timing and is unstable beyond 62 º BTDC fuel injection timing. The exhaust backpressure was maintained at 240 kpa with a tri-charged boost of CR20. The diesel supply was set at 3.8 g/min, and the measurement accuracy data is shown in **Table. 4.** To identify knock limits, engine knock tests were conducted at full load conventional and tri-charged engines at maximum compression ratio of 20. The cylinder peak pressure was found 72.3 bar at 52 cylinder volume at tri-charged mode CR20. Combustion ends at 20 º ATDC, 2.33 kJ heat release at 201 º ATDC and net heat release at 78 J/deg. The gas temperature was recorded at 1358 ºC in a tri-charged engine at 1.6 bar pressure shown in **Fig.14.**

**Figure 15. Variation of Heat Release Rate**

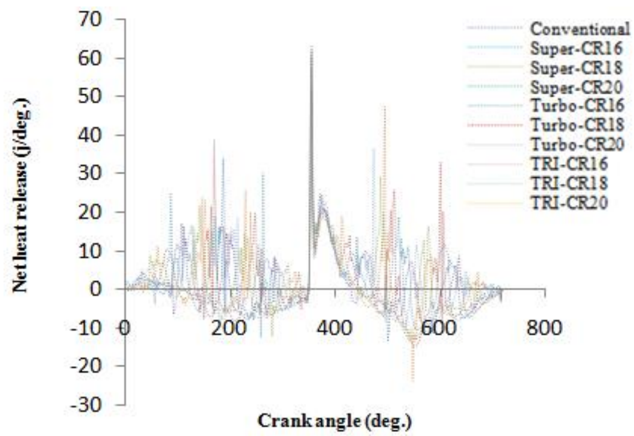


**Fig. 15** shows the heat release rate concerning crank rotation at different operating conditions of load and pressure. The highest heat release peak, the more advanced start of heat release, which result increase fuel conversion efficiencies. The HRR of the conventional engine was found at 6 º BTDC, which is around same for super, turbo, CR16 mode, whereas 1-2 º advances at tri-charged CR18. The maximum HRR is observed at tri-charged CR-20. The start of heat release at 4º CA and is 63 J/deg from increasing boost pressure at tri-charged, BTDC at tri-charged engine operating condition for compression ratio 18 to 20.

## 6. Conclusions

The present study compares a naturally aspirated engine performance and emissions with supercharged, turbocharged, and tri-charged mode at different compression ratios. An experimental trial was carried out to analyze and understand the combustion, performance and emission. From the results obtained following conclusions were made.

- As the orifice valve position of the tri-charger and quantity of fuel increase, the intake pressure and airflow rate increase. However, the efficiency of the compressor decreases because the compression ratio approaches the surge line, this result in a reduction in engine efficiency
- Due to combined tri-charging, the combustion pressure increased, which is why IMEP and BMEP increased. However, BSFC reduced from 0.33 Kg/kWh to 0.31 Kg/kWh at tri-charged CR18 operating conditions compared to conventional engine operating at CR 18. Some optimization is needed considering the correlation with an engine to improve performance.
- If an optimized compression ratio and tri-charged boost air are maintained, CO and HC are reduced. This is possible when there is fuel atomization by increasing the swirl motion in the combustion chamber by increasing boost airflow charge into intake due to tri-charged technology.
- The tri-charged technology is a fissile solution to power consumption by the supercharger and turbo-lag by the turbocharger as it provides initial power to turbocharger from the crank driven supercharger. However, there is a need to find the overall power produced and consumption by the tri-charged

- In order to improve the performance and reduce emissions, a tri-charged technology gives better results at a compression ratio of 18 with optimized boost air.
- The use of tri-charged at PPO-20 boost pressure tends to highest brake thermal efficiency at the engine's half and full load capacity.
- Thus, in real-life applications, using tri-charged technology at a compression ratio of 18 would be more beneficial for the engine performance at part and full load capacity.

In this study, the change in engine emissions and efficiency of diesel engines at a compression ratio of 18 is analyzed and compared with a tri-charger, which combines a crank driven supercharger, a turbocharger and electric supercharger, which was not investigated out in the previous study. Operating the tri-charger and adjusting airflow quantity improves the engine load carrying capacity, and the tri-charged technology is expected to have good advantages concerning fuel efficiency and emissions. Based on the present study results, future studies should be conducted to improve engine efficiency by optimizing intake air flow rate and temperature.

**Acknowledgement**

The authors acknowledge Apex Innovations Pvt. Ltd Kupwada, Sangli, Maharastra, India, to provide research facilities for the successful completion of this study.

**Highlights of the Paper**

1. A tri-charged technology is the best solution over the problem of power consumption and turbo-lag.
2. A tri-charged technology can be implemented successfully on single cylinder four-stroke diesel engine.
3. Tri-charged technique improves the engine performance and reduced emissions.
4. The tri-charging boosting gives best performance when engine operates at 18 compression ratio.

**Nomenclature & Abbreviation**

| | |
|---|---|
| rpm | Rotation per minute |
| BSFC | Brake Specific Fuel Consumption (g/kWh) |
| BMEP | Brake Mean Effective Pressure (bar) |
| IMEP | Indicated Mean Effective Pressure (bar) |
| BTHE | Brake Thermal Efficiency (%) |
| VGT | Variable Geometric Turbocharger |
| EGR | Exhaust Gas Recirculation |
| A/F | Air Fuel Ratio |
| HP | High pressure |
| LP | Low pressure |
| BP | Brake Power |
| N | Speed (rpm) |
| CO | Carbon Monoxide |

| | |
|---|---|
| $CO_2$ | Carbon Dioxide |
| HC | Hydrocarbon |
| NOx | Nitric Oxide |
| VCR | Variable Compression Ratio |
| W | Load (Kg) |
| T1 | Temperature of inlet/ ambient air (°C) |
| T2 | Temperature of outlet gasses/ after compressor (°C) |
| T3 | Temperature of cooling water inlet (°C) |
| T4 | Temperature of cooling water outlet (°C) |
| T5 | Temperature inlet to calorimeter (°C) |
| T6 | Temperature outlet to calorimeter (°C) |
| F1 | Fuel flow rate |
| F2 | Air flow rate |
| F3 | Cooling water flow rate (Rotameter) |
| F4 | Exhaust gas flow rate (Calorimeter) |

**Subscripts**

| | |
|---|---|
| Super | Supercharger |
| Turbo | Turbocharger |
| EVs | Electric Vehicles |
| Lab | Laboratory |
| Vol | Volume |
| Psc | Crank driven Supercharger Pressure |
| Pse | Electric driven Supercharger Pressure |
| Pt | Turbocharger Pressure |

**Greek**

| | |
|---|---|
| $\gamma$ | Ratio of specific heat capacities, 1.4 for air |
| $\rho$ | density |
| P-$\theta$ | Pressure- Crank angle |

**References**

1. Anh Tuan Hoanga and Van Viet Pham “A study on a solution to reduce emissions by using hydrogen as an alternative fuel for a diesel engine integrated exhaust gas recirculation” AIP Conference Proceedings 2235, 020035 (2020) Published Online: 04 May 2020 ; https://doi.org/10.1063/5.0007492.
2. Jai Prakash, Pawan Vats, Amit Kumar Sharma, Dilip Ganguly, Gazala Habib “New Emission Inventory of Carbonaceous Aerosols from the On-road Transport Sector in India and its Implications for Direct Radiative Forcing over the Region” Aerosol and Air Quality Research, 20: 741–761, 2020, Taiwan Association for Aerosol Research, ISSN: 1680-8584 print / 2071-1409 onlinedoi: 10.4209/aaqr.2019.08.0393.
3. Galindo, J., Lujan, J., Climent, H., Guardiola, C., & Varnier, O. (2014). A New Model for Matching Advanced Boosting Systems to Automotive Diesel Engines. SAE International Journal of Engines,7(1), 131-144. Retrieved May 12, 2020, from www.jstor.org/stable/26277755

4. Huiyan Zhang a, Lei Shi a, Kangyao Deng a, *, Sheng Liu b, Zhenhuan Yang “Experiment investigation on the performance and regulation rule of two-stage turbocharged diesel engine for various altitudes operation”, Energy 192 (2020) 116653. https://doi.org/10.1016/j.energy.2019.11665
5. Romagnoli, G. Vorraro, S. Rajoo, C. Copeland, R. Martinez-Botas “Characterization of a supercharger as boosting & turbo-expansion device in sequential multi-stage systems”Energy Conversion and Management 136 (2017) 127–141, http://dx.doi.org/10.1016/j.enconman.2016.12.051
6. Zinner K. Supercharging of internal combustion engines: fundamentals, calculations, examples. Springer-Verlag; 1978.
7. Zunqing Zheng, Hao Feng, Bin Mao, Haifeng Liu, Mingfa Yao A theoretical and experimental study on the effects of parameters of two-stage turbocharging system on performance of a heavy-duty diesel engine Applied Thermal Engineering 129 (2018) 822–832. https://doi.org/10.1016/j.applthermaleng.2017.10.044
8. R. Sauersteina, R. Dabrowski, M. Becker, W. Bullmer, Regulated two-stage Turbocharging for Gasoline Engines, BorgWarner Turbo Systems, 2010.
9. Aki Grönman, Petri Sallinen, Juha Honkatukia, Jari Backman, Antti Uusitalo Design and experiments of two-stage intercooled electrically assisted turbocharger Energy Conversion and Management Volume 111, 1 March 2016, Pages 115-124 https://doi.org/10.1016/j.enconman.2015.12.055
10. Felke, T., Holland, S., and Raviram, S., "Integration of Component Design Data for Automotive Turbocharger with Vehicle Fault Model Using JA6268 Methodology," SAE Int. J. Passeng. Cars – Electron. Electr. Syst. 10(2):380-389, 2017, https://doi.org/10.4271/2017-01-1623.
11. N. Sathishkumar1, P. Premkumar2, A. Ruskin Bruce3, K. Pravinkumar4, P.L. Sudharsan Design and Analysis of an Impeller of a Turbocharger International Journal of Research and ReviewVol.7; Issue: 4; April2020 E-ISSN: 2349-9788; P-ISSN: 2454-2237
12. Feng, Y., Lu, Z., Wang, T., Cai, J. et al., "Effect of Supercharging on the Intake Flow Characteristics of a Swirl-Supported Engine," SAE Technical Paper 2020-01-0794, 2020
13. Chiong, M., Abas, M., Tan, F., Rajoo, S. et al., "Steady-State, Transient and WLTC Drive-Cycle Experimental Performance Comparison between Single-Scroll and Twin-Scroll Turbocharger Turbine," SAE Technical Paper 2019-01-0327, 2019, http://lup.lub.lu.se/record/90aa0369-8577-4269-89e3-3e8ffd5de9c0
14. Mattos, A , Gallo, W . (2019). A Study of the Influence of the Intercooled Turbocharger and Cooled EGR on the Performance Parameters of an Ethanol-fueled Engine. International Journal of Thermodynamics , 22 (3) , 149-157 . DOI: 10.5541/ijot.499892
15. Liu, S., & Zhang, Y. (2020). Research on the Integrated Intercooler Intake System of Turbocharged Diesel Engine. International Journal of Automotive Technology, 21(2), 339–349. doi:10.1007/s12239-020-0032-9.
16. S. Tripathi, S. Singh, K. Ahmad and A. Thakur, "Despite the Turbo-Lag, Turbochargers are preferred to Superchargers by the Manufacturers," 2019 International Conference on Automation, Computational and Technology Management (ICACTM), London, United Kingdom, 2019, pp. 577-581, doi: 10.1109/ICACTM.2019.8776681.

17. Ali Assi1, Bassel Chokor1, Mohamad Hammoud1, 2, Ali Hallal1, Ali AL Shaer1, and Bakri Abdulhay Reducing the Turbo Lag of a Fixed Geometry Turbocharger IJISET - International Journal of Innovative Science, Engineering & Technology, Vol. 4 Issue 1, January 2017 ISSN (Online) 2348 – 7968
18. Song, K., Upadhyay, D., Hu, L., and Xie, H., "An Assessment of the Impact of Exhaust Turbine Redesign, for Narrow VGT Operating Range, on the Performance of Diesel Engines with Assisted Turbocharger," SAE Technical Paper 2019-01-0326, 2019, https://doi.org/10.4271/2019-01-0326.
19. Samoilenko, D., Marchenko, A. & Cho, H.M. Improvement of torque and power characteristics of V-type diesel engine applying new design of Variable geometry turbocharger (VGT). J Mech Sci Technol31, 5021–5027 (2017). https://doi.org/10.1007/s12206-017-0950-2.
20. Datla, R., Puli, R.K., Velayudhan Parvathy, C. et al. Effect of start of main injection timing on performance, emission, and combustion characteristics of a VGT CI engine fueled with neem biodiesel. Environ Sci Pollut Res (2020). https://doi.org/10.1007/s11356-020-08231-3.
21. Tian, W.; Du, D.; Li, J.; Han, Z.; Yu, W. Establishment of a Two-Stage Turbocharging System Model and Analysis on Influence Rules of Key Parameters. Energies2020, 13, 1953.
22. Huiyan Zhanga, Lei Shia, Kangyao Denga, Sheng Liub, ZhenhuanYangb Experiment investigation on the performance and regulation rule of two-stage turbocharged diesel engine for various altitudes operation Energy Volume 192, 1 February 2020, 116653. https://doi.org/10.1016/j.energy.2019.116653
23. Mohsen Mardi K a, Shahram Khalilarya a, Arash Nemati b,⇑ A numerical investigation on the influence of EGR in a superchargedSI engine fueled with gasoline and alternative fuels Energy Conversion and Management 83 (2014) 260–269. http://dx.doi.org/10.1016/j.enconman.2014.03.031
24. Amin Reihania,b, John Hoarda, Stefan Klinkertc, Chih-Kuang Kuanc, Daniel Stylesc, Greg McConvillec Experimental response surface study of the effects of low-pressure exhaust gas recirculation mixing on turbocharger compressor performance Applied Energy 261 (2020) 114349https://doi.org/10.1016/j.apenergy.2019.114349
25. Dawei Wanga, Lei Shia, Sipeng Zhua, Bo Liub, Yuehua Qianb, Kangyao Denga Numerical and thermodynamic study on effects of high and low pressure exhaust gas recirculation on turbocharged marine low-speed engine Applied Energy 261 (2020) 114346. https://doi.org/10.1016/j.apenergy.2019.114346
26. Koebel M, Elsener M, Marti T. NOx-reduction in diesel exhaust gas with urea and selective catalytic reduction. Combust Sci Technol 1996;121:85–102. https://doi. org/10.1080/00102209608935588
27. Agarwal D, Singh SK, Agarwal AK. Effect of Exhaust Gas Recirculation (EGR) on performance, emissions, deposits and durability of a constant speed compression ignition engine. Appl Energy 2011;88:2900–7. https://doi.org/10.1016/j.apenergy. 2011.01.066.
28. Baek, S., Woo, S., Kim, Y., & Lee, K. (2019). Prediction of turbocharged diesel engine performance equipped with an electric supercharger using 1D simulation. Energy, 185, 213–228. doi:10.1016/j.energy.2019.07.060
29. W. Lee, E. Schubert, Y. Li, S. Li, D. Bobba and B. Sarlioglu, "Overview of Electric Turbocharger

and Supercharger for Downsized Internal Combustion Engines," in IEEE Transactions on Transportation Electrification, vol. 3, no. 1, pp. 36-47, March 2017, doi: 10.1109/TTE.2016.2620172

30. Accurso, F., Zanelli, A., Rolando, L., and Millo, F., "Real Time Energy Management Control Strategies for an Electrically Supercharged Gasoline Hybrid Vehicle," SAE Technical Paper 2020-01-1009, 2020, https://doi.org/10.4271/2020-01-1009.Baek, S.,
31. Rose ATJM, Akehurst S, Brace CJ. Modelling the performance of a continuously variable supercharger drive system. J Automob Eng 2011;225(10):1399–414. https://journals.sagepub.com/doi/abs/10.1177/0954407011406320
32. Hu B, Copeland C, Lu P, Akehurst S, Brace C, Turner JWG, et al. A new de-throttling concept in a twin-charged gasoline engine system. SAE Int J Eng 2015;8(4):1553–61.
33. V. Kumaresh and S.Madhan "Compound forced induction system: Twincharger" International Journal of Innovative Research in Science, Engineering and Technology, Volume 3, Special Issue 2, April 2014, pp 24-27
34. Zhu D, Zheng X, Asymmetric twin-scroll turbocharging in diesel engines for energy and emission improvement, Energy (2017), doi: 10.1016/j.energy.2017.07.17310.1016/j.energy.2017.07.173
35. Buchman, Michael R., Johnson, W. Brett, and Winter, Amos G. "Analyzing the Effect of Air Capacitor Turbocharging Single Cylinder Engines on Fuel Economy and Emissions Through Modeling and Experimentation." Proceedings of the ASME 2018 International Design Engineering Technical Conferences and Computers and Information in Engineering Conference. Volume 3: 20th International Conference on Advanced Vehicle Technologies; 15th International Conference on Design Education. Quebec City, Quebec, Canada. August 26–29, 2018. V003T01A043. ASME. https://doi.org/10.1115/DETC2018-85934
36. Galindo, José, et al. "A New Model for Matching Advanced Boosting Systems to Automotive Diesel Engines." SAE International Journal of Engines, vol. 7, no. 1, 2014, pp. 131–144. JSTOR,www.jstor.org/stable/26277755. Accessed 12 May 2020.
37. Koniuszy A, Kostencki P, Berger A, Golimowski W. Power performance of farm tractor in field operations. Eksploatacja i Niezawodnosc – Maintenance and Reliability 2017; 19 (1): 43–47,http://dx.doi.org/10.17531/ein.2017.1.6.
38. Xiong, Rui, Quanqing Yu, and Cheng Lin. "A novel method to obtain the open circuit voltage for the state of charge of lithium ion batteries in electric vehicles by using H infinity filter." Applied energy 207 (2017): 346-353
39. k Sreeram ; P K Preetha ; Prabaharan Poornachandran Electric Vehicle Scenario in India: Roadmap, Challenges and Opportunities 2019 IEEE International Conference on Electrical, Computer and Communication Technologies (ICECCT) 19065336 DOI:10.1109/ICECCT.2019.8869479
40. J.Jaguemont, L.Boulon, Y.Dubé, A comprehensive review of lithium-ion batteries used in hybrid and electric vehicles at cold temperatures Applied Energy Volume 164, 15 February 2016, Pages 99-114https://doi.org/10.1016/j.apenergy.2015.11.034
41. García, A., Monsalve-Serrano, J., Martínez-Boggio, S., & Wittek, K. (2020). Potential of hybrid powertrains in a variable compression ratio downsized turbocharged VVA Spark Ignition

engine. Energy, 195, 117039. doi:10.1016/j.energy.2020.117039

42. Rychter TJ, Teodorczyk A, Stone CR, Leonard HJ, Ladommatos N, Charlton SJ. A Theoretical Study of a Variable Compression Ratio Turbocharged Diesel Engine. Proceedings of the Institution of Mechanical Engineers, Part A: Journal of Power and Energy. 1992; 206(4): 227-238. doi:10.1243/PIME_PROC_1992_206_039_02
43. Umesh, K. S., V. K. Pravin, and K. Rajagopal. "Experimental Investigation and CFD Analysis of Multi-Cylinder Four Stroke SI Engine Exhaust Manifold for Optimal Geometry to Reduce Back Pressure and to Improve Fuel Efficiency." International Journal of Automobile Engineering Research and Development, 4, 13 20 (2014).
44. Rani, Annepu Shobha, et al. "Experimental investigation on the performance and emission characteristics of di-diesel engine using diesel-ethanol blends and aluminium oxide nano particles." Int J Mech Product Eng Res Dev 7.5 (2017): 301-310.